

## The Phasor Approach to Fluorescence Lifetime Imaging Analysis

Michelle A. Digman,\* Valeria R. Caiolfa,<sup>††</sup> Moreno Zamai,<sup>††</sup> and Enrico Gratton\*

\*Laboratory for Fluorescence Dynamics, Department of Biomedical Engineering, University of California, Irvine, California; <sup>†</sup>Department of Molecular Biology and Functional Genomics, San Raffaele Scientific Institute, Milan, Italy; and <sup>‡</sup>IIT Network Research, Unit of Molecular Neuroscience, San Raffaele Scientific Institute, Milan, Italy

**ABSTRACT** Changing the data representation from the classical time delay histogram to the phasor representation provides a global view of the fluorescence decay at each pixel of an image. In the phasor representation we can easily recognize the presence of different molecular species in a pixel or the occurrence of fluorescence resonance energy transfer. The analysis of the fluorescence lifetime imaging microscopy (FLIM) data in the phasor space is done observing clustering of pixels values in specific regions of the phasor plot rather than by fitting the fluorescence decay using exponentials. The analysis is instantaneous since is not based on calculations or nonlinear fitting. The phasor approach has the potential to simplify the way data are analyzed in FLIM, paving the way for the analysis of large data sets and, in general, making the FLIM technique accessible to the nonexpert in spectroscopy and data analysis.

Received for publication 18 August 2007 and in final form 17 September 2007.

Address reprint requests and inquiries to Enrico Gratton, E-mail: egratton22@yahoo.com.

In fluorescence experiments multiple lifetime components arise from different molecular species or different conformations of the same molecule (1,2). Changes of lifetime values are interpreted in terms of molecular interactions (3,4). The measurement of the fluorescence decay in fluorescence lifetime imaging microscopy (FLIM) can be performed using several methods: the time-correlated single photon counting (5), the frequency-domain, and the time-sampling approach (6–8). One difference between FLIM and cuvette measurements is that in FLIM, only a few photons (~1000) are collected per pixel (9). This is barely enough to distinguish a single from a double exponential decay, which is required to determine if two species are present in the same pixel.

The analysis of FLIM data collected in the time domain proceeds by fitting the decay at each pixel using one or two exponentials and identifying decay times and amplitudes with molecular species and their relative abundances. A problem with this approach is that many of the fluorescent proteins used in microscopy display a complex decay behavior (10). Another problem with exponentials is that there is correlation between amplitude and characteristic exponential times. The analysis of the decay at each pixel (~10<sup>5</sup> pixels in an image) in using exponentials is a formidable computational problem that requires expertise to correctly extract the information about the number and abundance of the molecular species (11,12).

The phasor approach presented here has the potential of simplifying the analysis of FLIM images, avoiding some of the problems of the exponential analysis and providing a graphical global view of the processes affecting the fluorescence decay occurring at each pixel (8,13,14). To emphasize the novelty of the approach and to demonstrate that the phasor concept is not unique to the frequency domain, in this letter we use data collected with the time-correlated single

photon counting method. We also show that quantitative evaluation of fluorescence resonance energy transfer (FRET) efficiencies in the phasor plot does not require fitting exponentials.

The phasor method transforms the histogram of the time delays at each pixel in a phasor, which is like a vector (Supplementary Eq. 1, Supplementary Material). The values of the sine-cosine transforms are represented in a polar plot as a two-dimensional histogram (phasor plot). Each pixel of the image gives a point in the phasor plot. The phasor plot is also used in a reciprocal mode in which each (occupied) point of the phasor plot can be mapped to a pixel of the image. Since every molecular species has a specific phasor, we can identify molecules by their position in the phasor plot.

In Fig. 1, the precision of the determination of the phasors of cyan fluorescent protein (CFP), yellow fluorescent protein (YFP), and enhanced green fluorescent protein (EGFP) is sufficient to identify their origin. The resolution of phasors depends on the counts in each pixel (see figure caption). The phasors corresponding to fibronectin background and to cellular autofluorescence are spread over a larger area due to the low intensity (fibronectin) and to pixel heterogeneity (cellular autofluorescence). The phasor of the Raichu-Rac1 construct is also spread along a "trajectory" due to different amounts of FRET.

The rule of phasor addition (which is the same as the vector addition with normalization; Supplementary Eq. 4, Supplementary Material) helps in identifying the origin of points in a phasor cluster. If two molecular species are coexisting in the same pixel, all possible weighting of the two species give

Editor: Michael Edidin.

© 2008 by the Biophysical Society  
doi: 10.1529/biophysj.107.120154

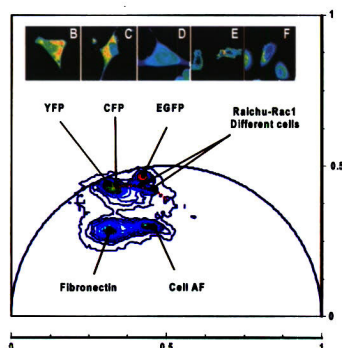


FIGURE 1 (A) Phasor plot of the FLIM images shown above. Transfected cells are: (B) CHO-K1 with YFP (306); (C) MEF with paxillin-CFP (442); (D) CHO-K1 with EGFP (1537); and (E) CHO-K1 with the RAICHU-Rac1 construct (665). (F) Untransfected cells to measure phasor of cell autofluorescence and fibronectin (573). The numbers in parenthesis indicate counts of the brightest pixel. The red dashed line corresponds to one possible FRET trajectory passing through the clusters of phasors corresponding to cells in the field of view.

phasors distributed along a straight line joining the phasors of the two species. In the case of three molecular species, the possible realizations of the system fill a triangle where the vertices correspond to the phasors of the pure species. Just observing the clustering of points in the phasor plot is sufficient to determine that some pixels of the image contain two (or more) molecular species. The relative fluorescence of the species can be obtained in a quantitative way using the "phasor calculator" that graphically implements Supplementary Eq. 4.

Fig. 2 shows the image of a CHO-K1 cell expressing paxillin-EGFP in a three-dimensional collagen matrix and of a region of the collagen matrix. The collagen fibers display very weak fluorescence with a very short lifetime (different from zero). The pixels that contain a combination of EGFP (1) and collagen emission (2) distribute along a line joining the phasors of the EGFP and collagen. The segment joining the phasor of EGFP and collagen is plotted. As the operator moves the cursor along the segment, the calculator (that solves Supplementary Eq. 4) displays the relative fractional contribution of the two components.

For interacting species (e.g., FRET pair) in which the presence of the acceptor reduces the lifetime of the donor, the resulting phasor of the interacting species cannot lie in the line joining the phasor of the two noninteracting species, but will be in a different part of the phasor plot corresponding to the quenched donor. For FRET the information about the molecular interaction is obtained by localizing the position of clusters of phasor in the phasor plot rather than by resolving

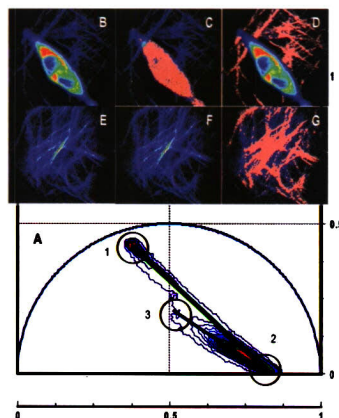


FIGURE 2 CHO-K1 cells transfected with paxillin EGFP in a three-dimensional collagen matrix. (A) Phasor plot of the two images. Region of the sample with a transfected cell (B) and with the collagen matrix (C). (D and E) Pixels in the image selected by the cursor at position 1 (EGFP) are highlighted in pink. (F and G) Pixels selected at position 2 (collagen). Position 3 represents weak background fluorescence. Pixels with multiple contributions lie along the line joining the EGFP and the collagen phasor (green line) or the background autofluorescence and the collagen phasor (black line). The cursor is used interactively to select a given cluster of phasors along the lines. The computer displays the relative contribution of the two species for each position of the cursor along the line.

the decay of the donor in exponential components. The quantitative information about the interaction (the FRET efficiency) can be obtained using the "FRET calculator" that implements graphically Supplementary Eqs. 4 and 5.

Fig. 3 shows images of cells transiently transfected with Cerulean (c) and Cerulean-Venus (c-v) constructs. The c-v complex display FRET due to the proximity of the two proteins. The FRET calculator is used to measure the FRET efficiency corresponding to the specific point along the FRET trajectory. The calculator also combines the phasor of the unquenched donor (c) and the phasor of the background (AF), which were determined independently using the c-only cell and a nontransfected cell. The amount of fluorescence of the donor and background to combine changes by the operator until the FRET trajectory passes through the experimental points in the phasor plot. The reciprocal property of the phasor cursor is illustrated in Fig. 3, C and E, which shows the correspondence of phasors that cluster in regions of the c-only phasors and of the c-v phasors (the pink highlighted regions).

Figs. 1–3 show that specific clustering of points in the phasor plot and along trajectories is sufficient to establish the physical origin of the changes in lifetime at different pixels.



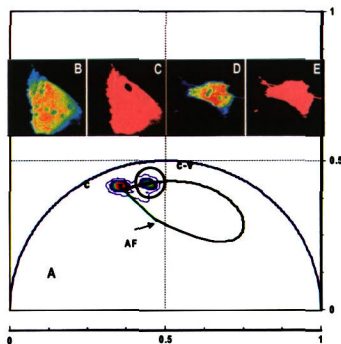


**FIGURE 3** MEF cells expressing cerulean and cerulean-venus constructs. (A) Phasor plot showing the clustering of phasors of cell B (c only) and (D) c-v construct. The curved trajectory corresponds to FRET efficiency (0–100%) and for a percentage of background and donor unquenched. The green line joins the phasor of the cerulean and the autofluorescence phasor, independently determined. The FRET efficiency at the cursor position is 0.208. The counts in the brightest pixels are 457 and 192 for the c-v and c-only cell, respectively. The fraction of background is 9.5% and the fraction of unquenched donors is 0.9%. Image C shows pixels selected at the position of the c-only cell and image E when the position of the cursor is as shown in A.

This is done without resolving the decay in exponential components, but by inspection of the phasor plot. The identification in the image where these processes occur is done using the reciprocal property of the phasor plot by which every point of the phasor plot can be identified with a pixel in the image.

Although no fits are performed, the exploration of the phasor plot using the cursor and the calculator provides quantitative results for several common situations such as combination of multiple decay components in a pixel (linear trajectories) and FRET (specific curved trajectories). The calculator approach in which the computer draws in the phasor plot the trajectories of selected processes allows full quantitation of the parameters of specific process.

In this letter we intentionally omitted the calculation of the “lifetime” of the phasor. We have shown that its knowledge is unnecessary to identify a specific molecular species (Fig. 1), to determine the fractional contributions of molecular species at one pixel (Fig. 2), or to calculate FRET efficiencies (Fig. 3). If the phasor falls on the universal circle (see Supplementary Material) it can be unequivocally associated with a lifetime value. If the phasor is not on the universal circle, the corresponding molecular species must have a complex decay. In this case, estimators of lifetime values can be obtained using phasor plots of higher Fourier harmonics. This subject has been discussed in the context frequency-domain fluorescence lifetime determinations and it is beyond the scope of this

article. Here we emphasize that the determination of lifetime components is unnecessary when the decay is represented in the phasor plot.

## SUPPLEMENTARY MATERIAL

To view all of the supplemental files associated with this article, visit [www.biophysj.org](http://www.biophysj.org).

## ACKNOWLEDGMENTS

We thank Dr. A. Horwitz and Dr. J. Schwartz for providing the RAICHU-RAC-1 and the Cerulean and Cerulean-Venus plasmids, respectively.

This work was supported in part by the Cell Migration Consortium U54 GM64346 (M.D. and E.G.), National Institutes of Health P41-RR03155 (E.G.), and the Ministero dell’Istruzione dell’Università e della Ricerca Italy FIRBBAU01CHJJ\_002 (V.R.C.). V.R.C. and M.Z. are grateful to the Cariplo Foundation (Milan, Italy) for confounding this work.

## REFERENCES and FOOTNOTES

- Wouters, F. S., P. J. Verveer, and P. I. Bastiaens. 2001. Imaging biochemistry inside cells. *Trends Cell Biol.* 11:203–211.
- Peter, M., and S. M. Ammer-Beg. 2004. Imaging molecular interactions by multiphoton FLIM. *Biol. Cell.* 96:231–236.
- Peyker, A., O. Rocks, and P. I. Bastiaens. 2005. Imaging activation of two Ras isoforms simultaneously in a single cell. *ChemBioChem.* 6:78–85.
- Peter, M., S. M. Ammer-Beg, M. K. Hughes, M. D. Keppler, S. Prag, M. Marsh, B. Vojnovic, and T. Ng. 2005. Multiphoton-FLIM quantification of the EGFP-mRFP1 FRET pair for localization of membrane receptor-kinase interactions. *Biophys. J.* 88:1224–1237.
- Becker, W., A. Bergmann, M. A. Hink, K. König, K. Benndorf, and C. Biskup. 2004. Fluorescence lifetime imaging by time-correlated single-photon counting. *Microsc. Res. Tech.* 63:58–66.
- Gerritsen, H. C., M. A. Asselbergs, A. V. Agronskaia, and W. G. Van Sark. 2002. Fluorescence lifetime imaging in scanning microscopes: acquisition speed, photon economy and lifetime resolution. *J. Microsc.* 206:218–224.
- Weber, G. 1981. Resolution of the fluorescence lifetimes in a heterogeneous system by phase and modulation measurements. *J. Phys. Chem.* 85:949–953.
- Jameson, D. M., E. Gratton, and R. Hall. 1984. The measurement and analysis of heterogeneous emissions by multifrequency phase and modulation fluorimetry. *Appl. Spectrosc. Rev.* 20:55–106.
- Gratton, E., S. Breusegem, J. Sutín, Q. Ruan, and N. Barry. 2003. Fluorescence lifetime imaging for the two-photon microscope: time-domain and frequency-domain methods. *J. Biomed. Opt.* 8:381–390.
- Suhling, K., J. Siegel, D. Phillips, P. M. French, S. Leveque-Fort, S. E. Webb, and D. M. Davis. 2002. Imaging the environment of green fluorescent protein. *Biophys. J.* 83:3589–3595.
- Verveer, P. J., A. Squire, and P. I. Bastiaens. 2000. Global analysis of fluorescence lifetime imaging microscopy data. *Biophys. J.* 78:2127–2137.
- Pelet, S., M. J. Previte, L. H. Laiho, and P. T. So. 2004. A fast global fitting algorithm for fluorescence lifetime imaging microscopy based on image segmentation. *Biophys. J.* 87:2807–2817.
- Clayton, A. H., Q. S. Hanley, and P. J. Verveer. 2004. Graphical representation and multicomponent analysis of single-frequency fluorescence lifetime imaging microscopy data. *J. Microsc.* 213:1–5.
- Redford, G. I., and R. M. Clegg. 2005. Polar plot representation for frequency-domain analysis of fluorescence lifetimes. *J. Fluoresc.* 15: 805–815.